Nanotubular-Aerogel/Hydrogel Hybrid for Strain Sensing Applications

*Qian Zhang,[a,b] Wenchao Ye,[a,b] Guojiao Li,[b] Yanli Gong,[a,b] Wenlang Liang *,[a,b] and Yongxiang Leng[a,b]*

[a] Institute of Biomedical Engineering, College of Medicine, Southwest Jiaotong University, Chengdu 610031, Sichuan, China

[b] Key Laboratory of Advanced Technologies of Materials, Ministry of Education and School of Materials Science and Engineering, Southwest Jiaotong University, Chengdu 610031, China

Table S1. Contents of samples

Sample	AA wt%	Py wt%	DDAB wt%
PPy Nanotubular-Aerogel	0	1	0
PAA Hydrogel	20	0	0.2
NAHH-1	10	1	0.2
NAHH-2	15	1	0.2
NAHH-3	20	1	0.2

Table S2. DDAB Concentrations used for antibacterial and biocompatibility experiments in NAHH-1

Sample	DDAB wt%
NAHH-$1_{DDAB\ 0\ wt\%}$	0
NAHH-$1_{DDAB\ 0.05\ wt\%}$	0.05
NAHH-$1_{DDAB\ 0.1\ wt\%}$	0.1
NAHH-$1_{DDAB\ 0.2\ wt\%}$	0.2
NAHH-$1_{DDAB\ 0.4\ wt\%}$	0.4

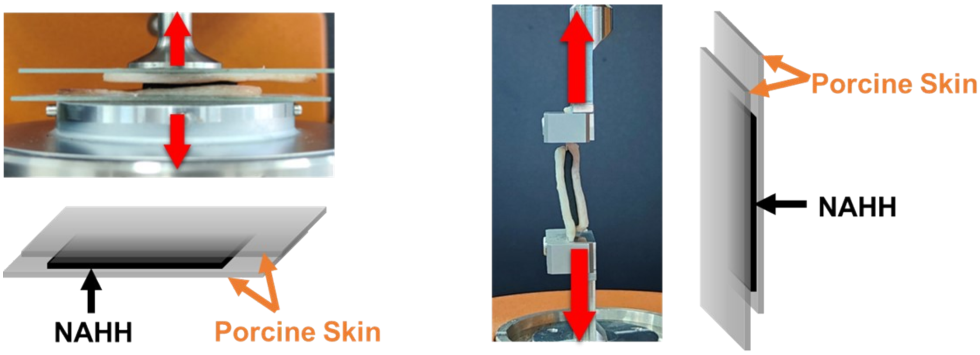

Figure S1. Tensile and shear adhesive strength measurement setups of the NAHH-1 on porcine skin, rubber and nitrile.

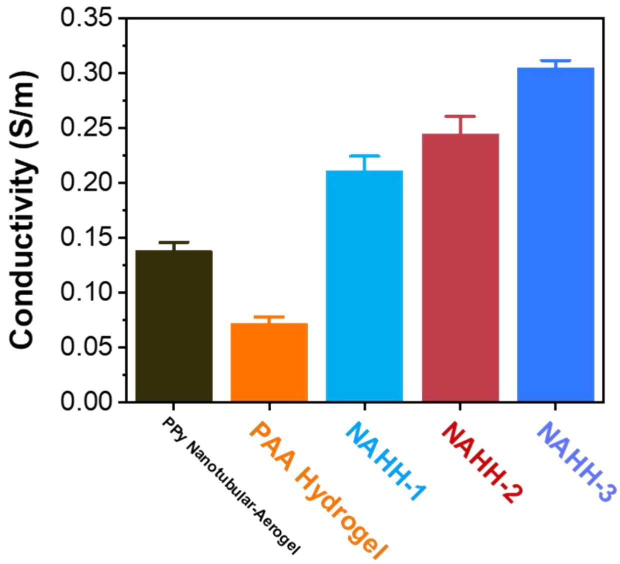

Figure S2. Conductivities of the PPy nanotubular-aerogel, PAA hydrogel, NAHH-1, NAHH-2 and NAHH-3.

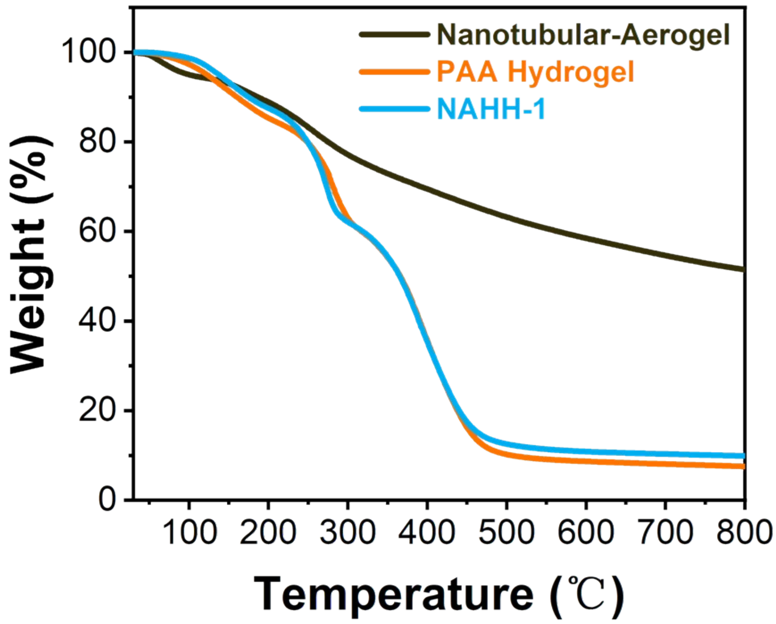

Figure S3. TGA of the PPy nanotubular-aerogel, PAA hydrogel and NAHH-1.

The thermal profile of the PPy nanotubular-aerogel revealed an initial weight reduction of approximately 6% up to 120°C, likely attributable to water evaporation (**Figure S3**). This was followed by a consistent weight loss of around 43% up to 800°C, leaving a residual mass of about 52%, a result that aligns with previous studies 1, 2. The PAA hydrogel underwent thermal degradation in two distinct stages, with weight losses occurring between 212-315°C and 315-480°C, leaving a mere 7% of the original mass at 800°C. The NAHH-1 displayed a similar two-phase weight loss to the PAA hydrogel, but its residual mass at 800°C (~10%) was intermediate between that of the PAA hydrogel and the PPy nanotubular-aerogel.

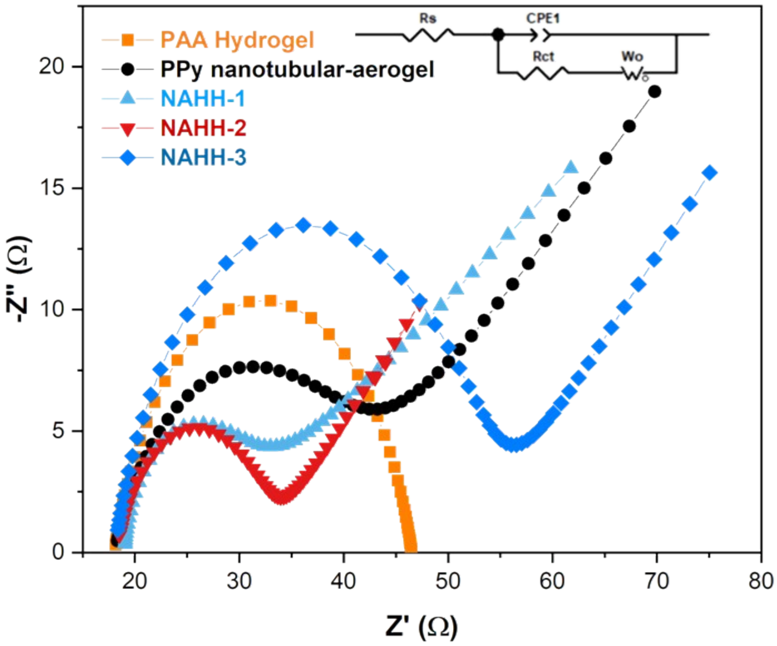

Figure S4. Nyquist diagram of PAA hydrogel, PPy nanotubular-aerogel, NAHH-1, NAHH-2 and NAHH-3 obtained through Electrical impedance spectroscopy (EIS) test.

Under ambient conditions, the samples were prepared in the cylindrical size with a diameter of 10mm and a height of 2mm, which were directly used as working electrodes. The experiments were conducted in a three-electrode electrochemical workstation (CorrTest CS Electrochemical Workstation) with an Ag/AgCl electrode as the reference electrode, a Pt sheet as the counter electrode, and a 1mol/L KCl aqueous solution as the electrolyte.

To further investigate the ion transport and capacitive behavior of the electrolyte, a Nyquist plot was obtained through Electrical impedance spectroscopy (EIS) testing in the frequency range of 10^5-0.1Hz (**Figure S4**). The inset in **Figure S4** shows the equivalent circuit diagram. As shown in the figure, the interception on the real axis represents the inherent resistance (R_s) of the hydrogel-electrode. The inherent resistances of PAA hydrogel, PPy nanotbulular-aerogel, NAHH-1, NAHH-2, and NAHH-3 are 18.164, 18.312, 19.059, 18.517, and 18.367Ω, respectively. In the mid-frequency region, the diameter of the semicircle corresponds to the interface transfer resistance (R_{ct}) between the electrode and the electrolyte. The interface transfer resistances of PAA hydrogel, PPy nanotubular-aerogel, NAHH-1, NAHH-2, and NAHH-3 are 28.334, 27.252, 15.076, 15.716, and 39.225Ω, respectively. Among them, NAHH-3 has the largest interface transfer resistance, and NAHH-1 has the smallest. In the low-frequency region, the linear relationship of the hydrogel-electrode, except for the PAA hydrogel-electrode, represents the Warburg impedance. The slopes of PPy nanotubular aerogel, NAHH-1, NAHH-2, and NAHH-3 are calculated to be 1.9, 2.3, 1.8, and 1.6, respectively. Among them, NAHH-1 has the smallest Warburg impedance, and NAHH-3 has the largest. This reflects the charge diffusion process and ideal capacitive behavior of the gelelectrode, which is close to the behavior of a double-layer capacitor. This Nyquist plot proves that the synthesized double network hydrogel possesses capacitive characteristics [3-5].

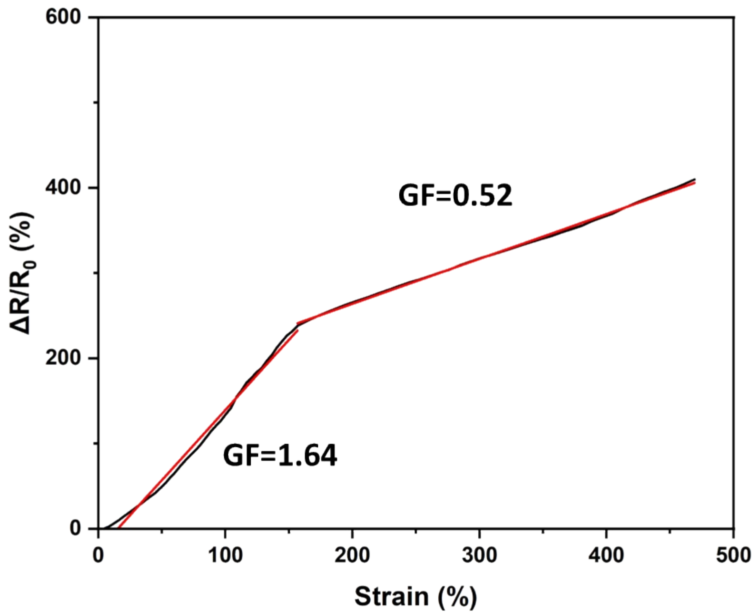

Figure S5. Electromechanical characteristics of NAHH-1.

During elongation or compression, the conductive networks of PPy nanotubules within the matrix undergo reorientation and rearrangement. Stretching causes the PPy nanotubules to separate within the elastomeric matrix, leading to an increase in electrical resistance. However, upon relaxation, the PPy nanotubules reposition, restoring the original resistance value at zero strain. Compression results in the collapse of the conductive networks, causing the PPy nanotubules to buckle or converge, thereby increasing the total number of conduction paths and facilitating electron transfer in the network. This process lowers the resistance by forming new contact points between PPy nanotubules. Once the load is removed, the electrical resistance reverts to its original value as the deformation of the PPy nanotubules fully recovers and the newly formed contacts cease to exist. The sensitivity of the NAHH-1, represented by the Gauge Factor (GF), is divided into two stages based on the strains. The GF is 1.64 in the range of 0-160% strain, and it decreases to 0.52 in the range of 160-470% strain (**Figure S5**).

References:

1. D. Muller, C. R. Rambo, L. M. Porto, W. H. Schreiner and G. M. Barra, *Carbohydr Polym*, 2013, **94**, 655-662.
2. Q. Wang, J. Zeng, J. Li, S. Yu, M. T. Innocent, M. Li, W. Ma, H. Xiang and M. Zhu, *Advanced Composites and Hybrid Materials*, 2022, **6**, 583-592.
3. L. Zhang, Y. Wu, Y. Xia and L. Jin, *Electrochimica Acta*, 2022, **412**, 140108.
4. X. Zhang, J. Zhao, T. Xia, Q. Li, C. Ao, Q. Wang, W. Zhang, C. Lu and Y. Deng, *Energy Storage Materials*, 2020, **31**, 135-145.
5. Y. Cheng, X. Ren, L. Duan and G. Gao, *Journal of Materials Chemistry C*, 2020, **8**, 8234-8242.